

Stress-strain behaviour of strain-hardening cement-based composites (SHCC) under repeated tensile loading

V. Mechtcherine & P. Jun

Technische Universitaet Dresden, Institute for Building Materials, Dresden, Germany

ABSTRACT: This paper presents results of an experimental investigation on the behaviour of strain hardening cement-based composites (SHCC) subjected to cyclic tensile loading. A series of uniaxial tensile tests on unnotched, dog-bone shaped prisms containing 2.25% by volume of polymeric fibre were performed using both a deformation and load control testing regime, respectively. The experimental program was replenished by a number of deformation controlled monotonic tensile tests as well as tensile creep tests. Two different specimen sizes were used. The effect of the curing conditions before testing was also investigated. The results obtained from the deformation controlled tests revealed no pronounced effect of the cyclic loading on the material performance for the number of loading cycles chosen. However, cracked specimens tested under the load control regime were more prone to failure at lower strain levels. The number of loading cycles prior to failure was considerably larger in comparison to the deformation controlled cyclic tests.

1 INTRODUCTION

This paper addresses the group of fibre reinforced cement-based composites (SHCC) which exhibit strain hardening, quasi-ductile behaviour due to the bridging of fine multiple cracks by short, well distributed fibres. The characteristic behaviour of SHCC in tension under monotonic, quasi-static loading was studied intensively during the last few years; see e.g. Mechtcherine & Schulze (2005), Mechtcherine & Schulze (2006). However, in practice, the majority of concrete structures is exposed to more or less severe cyclic loadings, such as traffic loads, temperature changes, wind gusts and in some cases sea waves, vibrations due to the operation of machinery or, in extreme circumstances, earthquake. Therefore, a profound knowledge of the fatigue behaviour of SHCC is indispensable for a safe and economical design of structural members, as well as building elements for which such materials might be used.

As of yet, only a few investigations on SHCC behaviour under cyclic loading have been performed. Fukuyama et al. (2002) investigated the cyclic tension-compression behaviour of two SHCC materials, which possessed a strain capacity of 0.5% and 1.0%, respectively; only about five cycles were needed until the strain capacity expired, while the cyclic tension response accurately reflected the corresponding curve obtained from a monotonic tension test. In contrast to this result, Douglas & Billington (2006) found that the envelop stress-strain curve from the

cyclic tests laid below the relation as measured in the monotonic regime. The difference was particularly pronounced in the experiments with high strain rates. The investigated SHCC showed a strain capacity of approximately 0.5% when subjected to monotonic, quasi-static loading.

Jun and Mechtcherine (2007) investigated an SHCC with a strain capacity that was clearly above 2% in all tests. A higher number of loading cycles was used compared to earlier studies. Furthermore, two different types of loading regimes were applied: deformation controlled and load controlled tests.

This paper presents results from a subsequent study in which additional test types (tensile creep tests) and test parameters (specimen size, curing conditions) were used. Results obtained will be presented and discussed in concert with previous results, and supplementary evaluation methods will be applied.

2 MATERIAL COMPOSITION

The characteristic behaviour of SHCC under monotonic tensile loading is shown in Figure 1 and can be described as follows. Microscopic defects trigger the formation of matrix cracks at so-called first crack stress (σ_1). As the first crack forms, the fibres bridge the crack transmitting tensile stresses across the crack surfaces. The applied load must be increased in order to enforce a further crack opening. This ac-

tion leads to the formation of another crack at the second weakest cross-section. The scenario then repeats resulting in a set of almost uniformly distributed cracks. The strain capacity is reached at the maximum load (tensile strength f_t), when the localisation of the failure occurs (one main crack develops). Due to a moderate opening of a large number of fine cracks, a strain capacity of several percent can be observed.

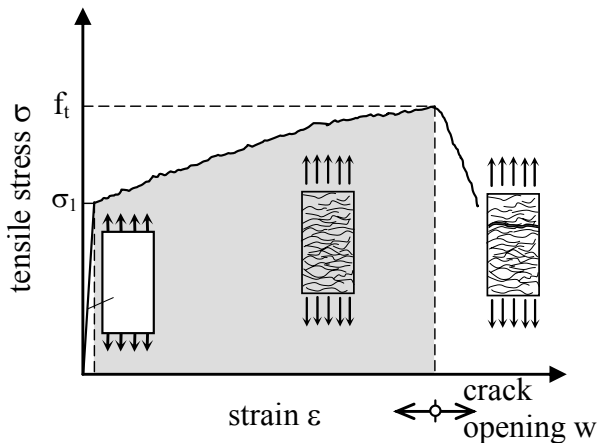


Figure 1. Typical stress-strain response and crack pattern of SHCC specimens under monotonic tensile loading.

SHCC, unlike common fibre reinforced concrete, is a micro-mechanically designed material. The approach for such material design was developed by Li (1993) for a composite which he called ECC (Engineered Cementitious Composite). The material used in this investigation was developed on the basis of this approach in earlier investigations by the authors; see e.g. Mechtcherine & Schulze (2005). However, a more specific term, SHCC, is used in this paper in conjunction with previous research conducted in this field.

Table 1 gives the SHCC composition used for the experiments. A mix containing a combination of Portland cement 42.5 R (30% by mass) and fly ash (70% by mass) was utilized as a binder. The fine aggregate was a uniformly graded silica sand with particle sizes of 0.06 mm to 0.20 mm. Furthermore, PVA fibres, 2.25% by volume with a length of 12 mm, were applied. A superplasticizer (SP) and a viscosity agent (VA) were added to the mix in order to adjust its rheological properties.

Table 1. SHCC composition used for the experiments.

Cement	Fly ash	Silica sand	Water	SP	VA	PVA fibres
[kg/m ³]						
321.0	749.1	535.0	334.5	16.6	3.2	29.3

The average compressive strength of the SHCC was 33.7 MPa. The compressive strength was derived from 12 displacement controlled tests on cubes with a side length of 100 mm. The displacement rate of the crosshead of the loading machine was 0.01 mm/s. The findings concerning the stress-strain curves obtained and the observed crack pattern will be published elsewhere.

3 TEST SET-UP, TESTING PROCEDURE AND EXPERIMENTAL PROGRAM

3.1 Specimen geometry, casting, curing, set-up

Based on the findings of previous investigations (Mechtcherine & Schulze, 2005 and Mechtcherine & Schulze, 2006), unnotched, dog-bone shaped prisms were chosen as specimens for this study. Such prisms were produced in two sizes, with identical geometrical shapes. The smaller prisms possessed a cross-section of 24 mm x 40 mm, while the larger ones had a cross-section of 60 mm x 100 mm. The gauge lengths were 100 mm and 250 mm, respectively. Figure 2 gives further geometric data for the specimens.

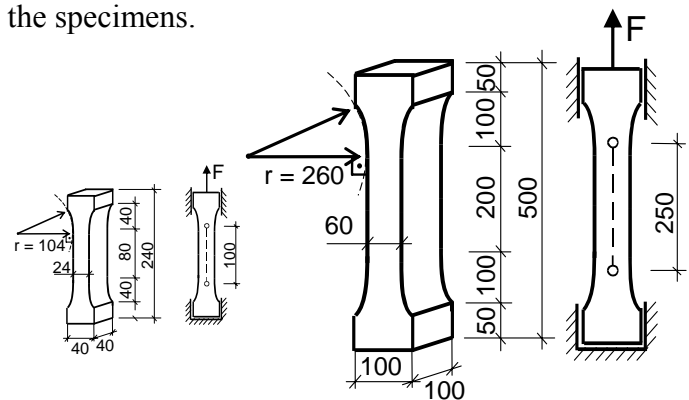


Figure 2. Geometry of the specimen used for the tensile tests.

All specimens were cast horizontally in metal forms. The moulds were stored 2 days in a climate box ($T = 25^{\circ}\text{C}$, $\text{RH} = 65\%$). After demoulding, the specimens were wrapped in a plastic foil (sealed condition) and stored until testing at room temperature. For some test series the specimens were stored after demoulding at the room atmosphere without any protection from desiccation (i.e. unsealed condition) in order to subsequently study on these specimens the effect of the curing conditions on the material performance under cyclic loading. All specimens were tested at a concrete age of 28 to 32 days.

The uniaxial tension tests were performed with non-rotatable boundaries. The deformations were measured by means of two LVDTs fixed to the specimen as displayed in Figure 3. The specimen surfaces were covered with a thin brittle white paint in order to facilitate monitoring of the crack's development.

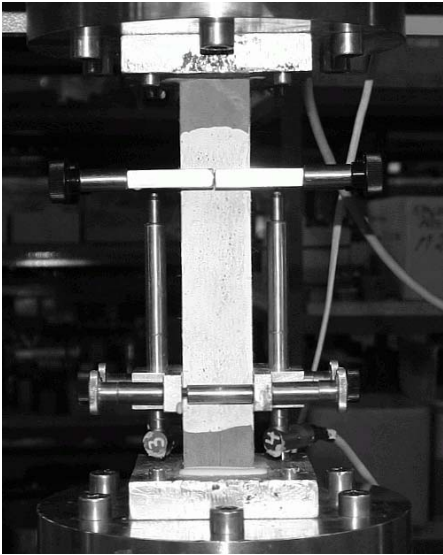


Figure 3. Used test set-up (here for small prisms).

3.2 Testing procedure

Four types of the experiments were performed with regard to the loading procedure: 1) monotonic deformation controlled tests; 2) cyclic deformation controlled tests; 3) cyclic load controlled tests, and 4) creep tests.

In the deformation controlled experiments, the deformation rate was always 0.01 mm/s which corresponds to a strain rate of 10^{-4} 1/s for the smaller prisms and $4 \cdot 10^{-5}$ 1/s for the larger specimens. For the deformation controlled cyclic tests the increase of the total deformation within the measuring length was given by the deformation increment $\Delta\delta$ which was chosen to be equal 0.1 mm for the small prisms and 0.25 mm for the large prisms (which corresponds to a strain increment of 0.1%) while being held constant from cycle to cycle. When the preset value $\Delta\delta$ in the following cycle was reached, the specimen was unloaded until the lower reversal point δ_{min} was attained. The lower reversal point δ_{min} was defined as a function of the lower load level $F_{min} = \text{const} = 0$ N.

In the load controlled cyclic tests, the specimen was first loaded monotonically until the strain value 0.5% was reached. The specimen was then unloaded and subsequently reloaded cyclically in a load control regime with predefined lower and upper load limits. The preloading in the monotonic regime was needed because of a pronounced scatter in first crack stress σ_I as had been observed in the monotonic tests. The knowledge of the behaviour of a particular specimen at the beginning of cracking enabled a purposeful choice of the upper stress limit σ_{up} for the cyclic loading. The lower limit was always set to $F_{min} = 0$ N, while the upper limit σ_{up} was chosen under careful consideration of the measured material behaviour during the initial monotonic loading regime.

Since the stress-strain curves under monotonic loading were generally rather unsteady in this investigation (see, for example, the curve shape given in

Figure 5b), the choice of the upper limit value σ_{up} was not straightforward. Basically, a stress value lying between the stress at first cracking σ_I and the maximum stress σ_{max} measured before changing to the load control was sought. However, in some cases, after the first cracking, a sudden stress drop occurred and the stress level at the strain of 0.5% was below the stress at first cracking σ_I . In such cases, the stress level after the stress drop due to the first cracking and subsequent “recover” was used instead of the σ_I value.

The load frequency in the load controlled cyclic tests was 0.5 Hz, i.e. each loading cycle took 2 seconds.

In the creep tests the specimens were also loaded monotonically until the strain value of 0.5% was reached. Once reached, the test control mode was switched to the load control regime. In order to derive the creep stress, the same procedure that was used to determine the upper limit value σ_{up} in the load controlled cyclic tests was also used for this procedure.

3.3 Overview of the experimental program

The results of two test series will be presented in the subsequent chapter. These following series, referred to as Series I and II, were performed with a time interval of a few months using the same SHCC composition. Despite the same production procedure, the mechanical performance of the specimens of Series II was somewhat different – in general, a lower tensile strength and a higher strain capacity – than those produced from Series I. A reason for this difference might be the usage of a new charge of the cement and fly-ash for the SHCC production. More comments relevant to this issue will be given in Chapter 4.

In Series I only the small prisms were tested, and all were stored under sealed condition until testing. Five specimens were tested for each loading condition (monotonic, cyclic deformation controlled and cyclic load controlled). Two specimens were subjected to sustained tensile loading for the creep test.

In Series II, four small prisms, stored unsealed after demoulding, were tested under the monotonic and deformation controlled regimes, respectively. Additionally, monotonic and cyclic tests (both deformation and load controlled) were performed on the large prisms. Two specimens were tested in each loading regime.

4 EXPERIMENTAL RESULTS

4.1 Behaviour under monotonic loading

The behaviour of the SHCC under monotonic tensile loading was studied in detail in earlier investigations (e.g. Mechtcherine & Schulze 2006). Therefore, the results from the monotonic tests obtained in this

study will be presented and discussed solely as a reference to the corresponding results from the cyclic tests. However, one general remark should be made with regard to the shape of the measured stress-strain curves. These curves display some sudden “jumps” and “drops” which were not experienced by the authors in the previous investigations using the same material composition (Mechtcherine & Schulze 2006). One reason for this peculiarity might be the change of the testing machine and the test control regime (the *displacement* of the machine cross-head was used in the earlier studies for the test control). The “new” machine – which was more appropriate for the cyclic tests – working in the deformation controlled regime evidently tended to “over-control” the tests in the instance of sudden stiffness changes due to the formation of new cracks. The unsteadiness of the stress-strain curves hampered the evaluation of the results to some degree, but, otherwise, did not seem to affect the information obtained from the experiments.

4.2 Results of deformation controlled cyclic tests

Figure 4 shows representative results from deformation controlled cyclic tests in comparison to the curves obtained using the monotonic loading regime. Nearly no effect of the given, relatively moderate number of loading cycles on the shape of the stress-strain diagram can be observed when considering only the envelope curves. This holds true for the experiments both with small and large prisms, as well as with sealed and unsealed specimens. The lack of a pronounced distinction in the envelope curve course naturally results in only minor differences in the average values of the stress at first cracking σ_1 , tensile strength f_t , as well as the strain capacity ε_{tu} , for these two different loading regimes; see Table 2.

The curves obtained from the cyclic tests show characteristic hystereses from which it can be clearly recognised that the high strains are to a great extent due to non-elastic deformations (see strains at zero stress). Furthermore, the stiffness of the composite gradually decreases (the inclination of the hysteresis curves with regard to the strain axis declines).

Table 3 gives values of the respective secant modulus of elasticity for several chosen strain levels. Tests with all three parameter combinations show a very pronounced decrease of this characteristic by a factor of approximately four, when the strain gradually increases from 0.5% to 3.0%.

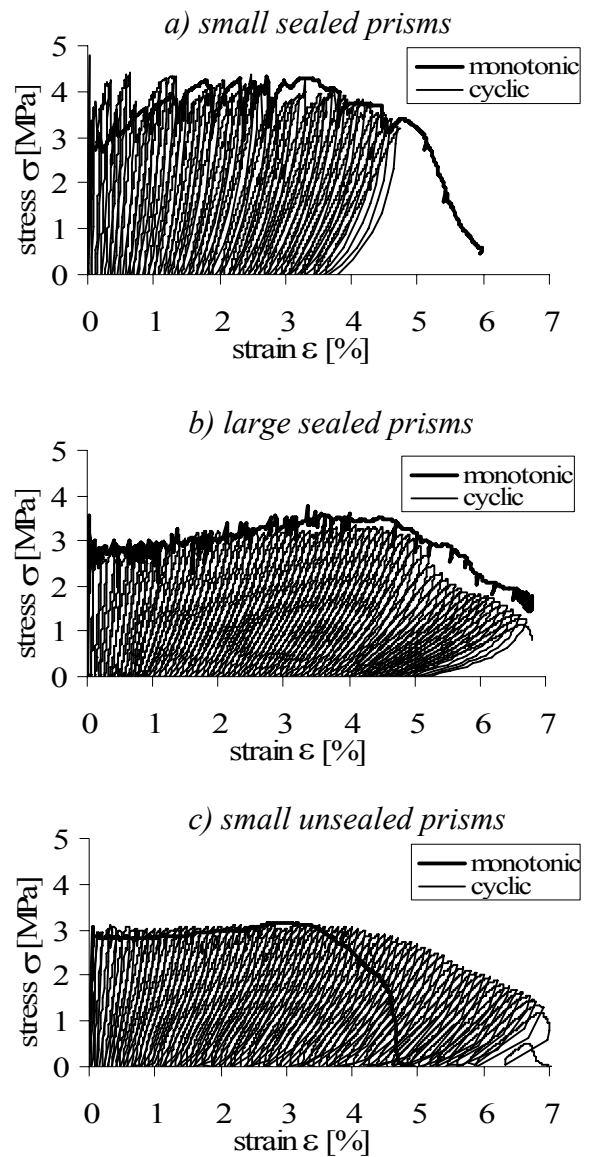


Figure 4. Representative results of the deformation controlled cyclic tests in comparison to the curves obtained using monotonic loading for: a) small sealed prisms, b) large sealed prisms, and c) small unsealed prisms.

A comparison of the stress-strain curves obtained for the small and large prisms, as well as the analysis of the derived characteristic values, show some discrepancy. The large prisms seem to provide a little smaller values of the first cracking stress level and the tensile strength, but they display a more apparent hardening and a higher strain capacity. This is in contrast to the results of an earlier investigation (Mechtcherine & Schulze 2005) in which an opposite tendency had been observed. However, unlike the cited investigation, in this study the large and small prisms were produced from different batches and with a time interval of several months. Therefore, the observed difference is evidently due to the minor changes of the raw materials used (see also Section 3.3).

Table 2. Statistical evaluation of the mechanical performance of the investigated SHCC for different loading regimes.

Type of loading	Number of cycles N [-]	Stress at first cracking σ_1 [MPa]	Tensile strength f_t [MPa]	Upper stress (l. con.) σ_{up} [MPa]	Strain capacity ϵ_{tu} [%]
Series I, small prisms, sealed, 5 specimens per loading type					
Monotonic, deform. controlled	1	3.6 (0.7)	4.7 (0.3)	-	2.5 (0.8)
Cyclic, deformation controlled	24 (6)	3.9 (0.7)	4.3 (0.1)	-	2.4 (0.6)
Cyclic, load controlled	1840 (1200)	3.4 (0.4)	3.9 (0.2)*	3.4 (0.3)	2.4 (0.3)
Creep	1	3.4 (-)*	3.9 (-)*	3.7 (-)	3.0 (-)
Series II, large prisms, sealed, 2 specimens per loading type					
Mon., def. control.	1	3.2 (-)	3.8 (-)	-	5.0 (-)
Cyc., def. control.	38 (-)	3.2 (-)	3.4 (-)	-	3.8 (-)
Cyc., load control.	2100 (-)	2.9 (-) *	3.1 (-) *	2.8 (-)	2.0 (-)
Series II, small prisms, unsealed, 4 specimens per load type					
Monotonic, def. control.	1	3.0 (0.4)	3.3 (0.5)	-	3.3 (0.4)
Cyclic, def. control.	42 (8)	3.1 (0.3)	2.9 (0.1)	-	4.2 (0.8)

* Values belong to the monotonic curves before changing to the load controlled regime.

(-) Only two measurements were performed.

A similar note should be made with regard to the apparent effect of the curing conditions in the tests on the small prisms. In previous studies, slightly lower values of the stress at the first cracking, the tensile strength and the strain capacity had been observed in the case of unsealed specimens. In the present study, the difference in the first two characteristic values was more pronounced, and the strain capacity was higher in the tests on the unsealed prisms. Minor changes of raw material might be the reason for such a discrepancy.

Remarkably, the curves obtained from the monotonic and cyclic tests on the specimens subjected to desiccation (i.e. unsealed ones) showed a much smoother shape of the stress-strain diagrams in comparison to those measured on the sealed specimens (compare Figures 4a and 4c). This can probably be traced back to the effect of the SHCC drying on the crack propagation in the specimen. Tensile eigenstresses develop at the surface vicinity due to a pronounced moisture gradient, causing formation of micro-cracks even before any mechanical loading is applied. As a result, when such a specimen is sub-

jected to a mechanical loading, the distribution of stresses over the specimen cross-section is highly non-uniform (i.e. at the surfaces much higher than in the middle). The cracks are prone to develop steadily from the surface into the interior of the prisms inducing no sudden stiffness changes unlike the case of the sealed specimens which has a more uniform stress field and, accordingly, a more spontaneous development of individual cracks.

Table 3. Change of the SHCC stiffness with increasing induced strain as observed in deformation controlled cyclic tests.

Strain under load	Large prisms	Small prisms	
		sealed	unsealed
	Secant modulus E [GPa]		
	Average value (standard deviation)		
0.5%	11.0 (-)	20.4 (3.1)	13.4 (2.8)
1.0%	8.1 (-)	14.3 (2.7)	6.0 (1.3)
1.5%	5.3 (-)	10.8 (2.2)	5.3 (0.6)
2.0%	5.1 (-)	8.0 (1.5)	4.1 (0.7)
3.0%	3.9 (-)	5.1 (1.4)	3.1 (0.3)

(-) Only two measurements were performed.

These suggestions can be confirmed by the analysis of the crack pattern; the cracks were mostly planar and usually propagated throughout the specimen in the case of the sealed prisms. The fracture surface after specimen failure was usually rather smooth, as well. On the contrary, the cracks observed at the surfaces of the unsealed prisms were usually not planar but rather had sophisticated patterns that did not continue throughout the entire specimen.

4.3 Results from load controlled cyclic tests

Figure 5 presents a typical stress-strain curve obtained from the load controlled cyclic tests. After switching to the load controlled regime at the strain of 0.5%, the individual hysteresis lie dense to each other and can hardly be recognized on the scale used. The shape of individual hysteresis for a few chosen strain levels will be presented and discussed in Section 4.5. On average, 1840 load cycles were needed to bring the specimen to failure in the case of the small specimens and 2100 cycles in the case of the large prisms.

In the tests on small prisms, which were performed in the frame of Series I, the strain capacity was practically the same as in the monotonic tests or the deformation controlled cyclic tests (see also Table 2). However, in Series II, the strain capacity obtained from the load controlled cyclic tests was clearly below the corresponding values for the deformation controlled monotonic or cyclic loading. This can be, at least partially, explained by the fact that the material could not relax after the formation of new cracks during the load controlled tests in contrast to the de-

formation controlled tests where the recurrent unloading took out a part of energy resealed due to cracking. Why this phenomenon was not observed in the tests on small prisms still need to be clarified.

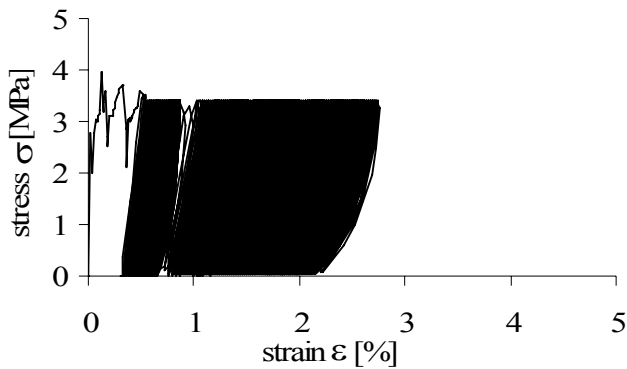


Figure 5. Representative stress-strain curves from the load controlled cyclic tests.

Table 4 gives values of the secant modulus of elasticity for several chosen strain levels. A pronounced decrease of the material stiffness can be stated in all tests. The degree of the stiffness reduction is similar to that obtained in the deformation controlled cyclic tests (cf. Table 3); however, on average the apparent stiffness seems to be higher in the load controlled tests. This can likely be traced back to a higher strain rate in these tests in comparison to the deformation controlled tests.

Table 4. Statistical evaluation of the load controlled tests, the secant modulus of elasticity.

Stage	Large prisms, sealed	Small prisms, unsealed	Small prisms, sealed
	Cyclic-load controlled		Creep
	Secant modulus E [GPa]		
	Average value (standard deviation)		
0.5% loaded	18.4**	17.1 (5.7)	16.7**
1.0% loaded	11.8**	13.6 (1.3)	10.5*
1.5% loaded	9.0**	9.9 (1.0)	-
2.0% loaded	7.4*	7.5 (0.8)	6.2*

* Only one measurement was performed

** Only two measurements were performed.

4.4 Results from creep tests

The tensile creep tests were only performed with small prisms that were sealed in foil until testing. Figure 6 shows a stress-strain relation obtained from one of the experiments performed which can be considered representative for both tests. The specimens were first loaded in the monotonic deformation control regime since the creep behaviour of cracked SHCC was the subject of interest. The portion of the curve recorded prior to the change to the load control regime at the strain of 0.5% is comparable to the curves obtained from monotonic tests.

In the creep regime, the load was kept constant, except for two or three intermediate unloading and reloading cycles which were performed in order to monitor the development of the material stiffness as a result of sustained tensile loading. This issue will be discussed in Section 4.5 together with the corresponding results from other tests.

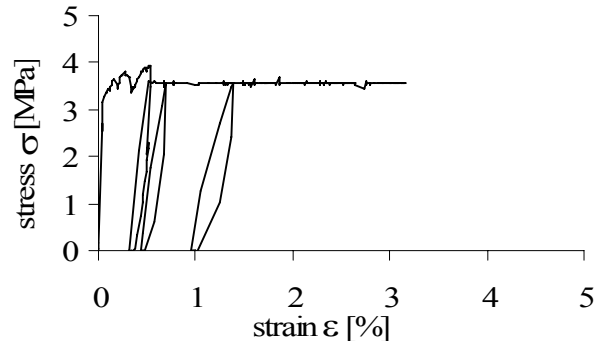


Figure 6. Representative stress-strain curve obtained from creep tests on small sealed prisms.

The strain capacity was found to be slightly higher by comparison to the corresponding deformation controlled tests (cf. Table 2). The time until failure was approximately 5 hours in the first test and approximately 16 hours in the second experiment. In two further tests (not evaluated here in detail), the change to the load control regime occurred at the strain of 1% and 2%, respectively. Higher strain capacity and considerably shorter time to failure were measured in these experiments.

4.5 Shape of the hysteresis in the cyclic tests

In previous sections, the secant modulus of elasticity was presented and discussed as an appropriate measure for the change of the SHCC stiffness resulting from repeated loading. The shape of the individual hysteresis of the stress-strain curves is another feature characterising the material response. This feature will be considered here for all loading regimes used.

Figure 7 shows representative shapes of the chosen individual cycles obtained from deformation controlled and load controlled tests on small sealed prisms. In both types of tests, material stiffness gradually decreases while the hysteresis loops become wider and rounder. The change of the loop shape is more pronounced for deformation controlled tests due to the fact that these contain a considerable portion of in-elastic deformation which increases with the increasing number of loading cycles. In contrast to this, only a very small portion of in-elastic deformation was recorded for the individual hysteresis loops in the load controlled cyclic tests. The SHCC behaviour in the individual load cycles can be described as nearly non-linear elastic. However, one can also observe a clear tendency of wider loops associated with higher strain levels.

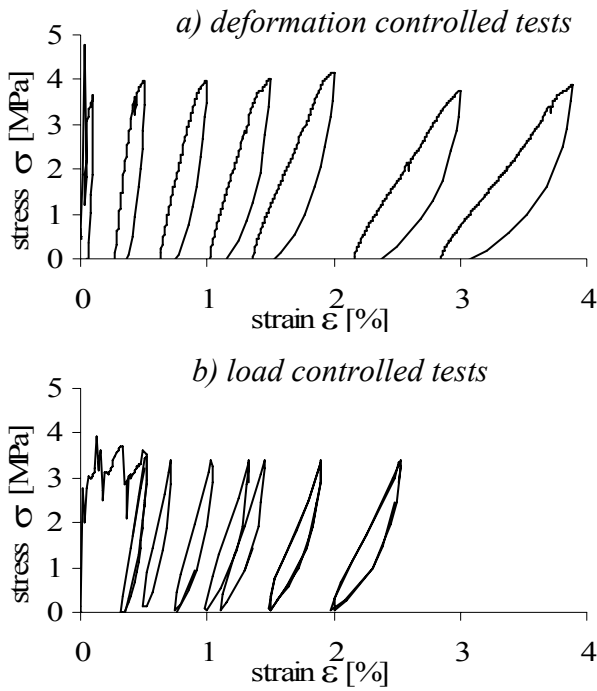


Figure 7. Representative shapes of the chosen individual cycles obtained from a) deformation controlled and b) load controlled tests on small sealed prisms.

It is worth noting that the shape of the un- and re-loading loops from the creep tests is similar to those obtained from the load controlled cyclic tests at the same strain levels. It is not surprising since the load control regime was applied for the creep tests, as well. The fact that the loops from the creep tests are slightly wider can be traced back to a lower un- and re-loading rate in these tests compared to the cyclic load controlled tests.

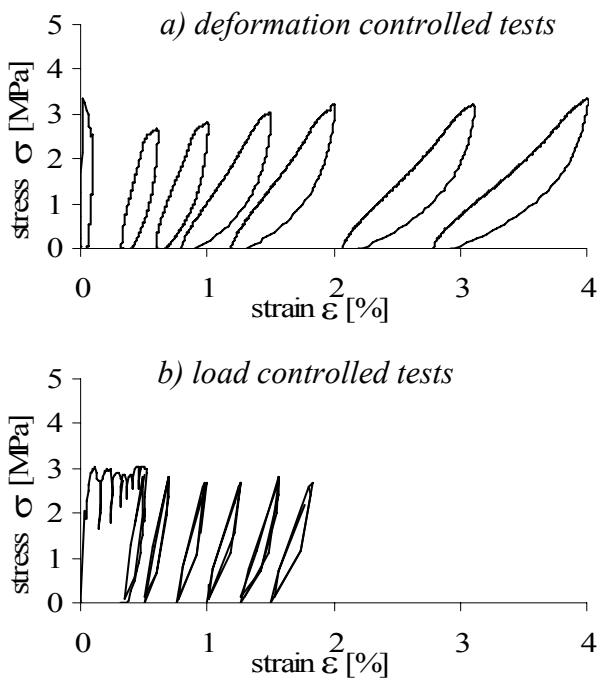


Figure 8. Representative shapes of the chosen individual cycles obtained from a) deformation controlled and b) load controlled tests on big sealed prisms.

The results from the cyclic tests on large prisms do not differ in essence from the results obtained for the small prisms (compare Figures 7 and 8). In the case of the deformation controlled tests, the loops of the stress-strain relations measured on the large prisms are more inclined and, at least for lower strain levels, wider than the corresponding hysteresis loops observed in the tests on the small prisms. A higher number of cracks per unit length of the specimen (cf. Table 5) provides a possible explanation to this phenomenon.

4.6 Comparison of the crack system

Development of the cracks on the specimen's surfaces was monitored during the tests; a number of high resolution digital photographs were taken at given strain levels and visually evaluated afterwards. Only cracks that propagated throughout the specimen were taken into account; no crack branches or one-sided cracks were taken into consideration. This restriction, however, strongly hampered the evaluation of the cracks observed on the small unsealed prisms. Due to pronounced micro-cracking on the specimen surfaces caused by drying, the cracks developed under loading were usually not planar but had complicated shapes and did not propagate throughout the entire specimen. As a result, fracture surfaces (final crack) were also very rough and not perpendicular to the load axis (cf. Figure 9). A more profound evaluation will be needed in order to appropriately describe the crack pattern and geometry in the unsealed prisms. For this reason, the results of these experiments under such curing conditions are not included in this paper.

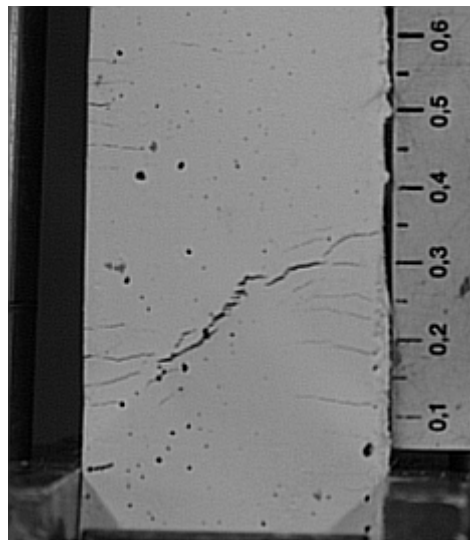


Figure 9. Typical failure pattern from the tests on small unsealed specimens.

Table 5 gives a statistical evaluation of the crack numbers observed in the different types of tests at the strain levels of 0.5%, 1.0% and 2.0%, respectively. For Series I of the tests, an evaluation of the

crack widths is given in Jun & Mechtcherine (2007). Series II results are still being completed.

Basically, the number of cracks increases with increasing strain level while the average and maximum crack widths become slightly larger (see Jun & Mechtcherine, 2007). Generally, the values do not differ much with regard to the loading regime. The deformation controlled cyclic tests provided on average fewer cracks with slightly larger crack openings in comparison to the other two types of tests conducted. More testing is needed in order to prove if this difference is statistically significant.

Table 5. Crack number comparison.

Specimen type	Type of loading	Strain ϵ [%]	Number of cracks n [-] average values (stand. deviation)
small prisms, sealed	monotonic	0.5	-
		1	8 (2)
		2	12 (3)
	cyclic, deformation controlled	0.5	4 (0)
		1	6 (1)
		2	9 (1)
	cyclic, load controlled	0.5	5 (1)
		1	8 (2)
		2	12 (2)
big prisms, sealed	monotonic	0.5	14* / 5.6**
		1	23* / 9.2**
		2	36* / 14.4**
	cyclic, deformation controlled	0.5	13* / 5.2**
		1	23* / 9.2**
		2	34* / 13.6**

* only one prism was considered, gauge length of 250 mm

** number of crack related to the reference length of 100 mm (i.e. the same gauge length as used in the tests on small prisms)

Table 5 provides the entire number of cracks counted, for the large prisms, over the gauge length used of 250 mm; this number is then divided by 2.5, in order to obtain a direct comparison with the results obtained from the small prisms (gauge length of 100 mm). The large and small prisms revealed similar crack development with increasing strain for both monotonic and cyclic loading; however, the crack density was higher in the case of large prisms. This higher density corresponds well with the higher strain capacity of the specimens tested in Series II (large sealed prisms) in comparison to Series I (small sealed prisms). A possible reason for this difference was discussed in Section 3.3.

5 CONCLUSIONS

The following conclusions can be drawn from the results obtained relative to the effect of the loading regime on the performance of the SHCC tested.

In the deformation controlled regime, the repeated loading caused a decrease in the tensile strength of SHCC compared with the results from the monotonic tests. However, there was no pronounced effect on the strain capacity of the material for the relatively small number of loading cycles applied. Further experiments are needed in order to study the influence of a larger number of loading cycles on the material behaviour.

There was no effect observed on the strain capacity from repeated loading for the tests on small specimens using a load control regime. However, there was a pronounced decrease of this material parameter in the tests involving large prisms. More tests are required in this area, as well.

The analysis of hystereses of the stress-strain curves showed a pronounced decrease of the material stiffness with an increasing number of loading cycles; the hysteresis loops became wider, as well. The hystereses obtained from the deformation controlled cyclic tests revealed a considerable inelastic deformation portion in every loop. The load controlled cyclic tests provided loop shapes which contained only minimal inelastic portion; however, due to a large number of load cycles in these tests, the accumulated inelastic deformations were comparable to those obtained from the deformation controlled tests for the same strain levels.

The number of cracks, as well as the crack widths, as observed on the specimen's surfaces did not vary much given the different loading conditions.

REFERENCES

- Douglas K.S. & Billington S.L. 2006. Rate-dependence in high-performance fiber-reinforced cement-based composites for seismic applications. *Int. RILEM Workshop on HPRCC in Structural Applications*, Honolulu, May 2005, G. Fischer & V. C. Li (eds.), RILEM Publications S.A.R.L., PRO 49: 17-26.
- Fukuyama, H. & Haruhiko, S., & Yang, I. 2002. HPRCC Damper for Structural Control. *Proceedings of the JCI International Workshop on Ductile Fiber Reinforced Cementitious Composites (DFRCC)*, Takayama, Japan, Japan Concrete Institute: 219-228.
- Jun, P. & Mechtcherine, V. 2007. Behaviour of strain-hardening cement-based composites (SHCC) under cyclic tensile loading. *International Conference CONSEC'07*, Tours, France, accepted for publication.
- Li, V. C. 1993. From micromechanics to structural engineering – The design of cementitious composites for civil engineering applications. *JSCE J. of Struc. Mechanics and Earthquake Engineering*. 10 (2): 37-48.
- Mechtcherine, V. & Schulze, J. 2005. Ultra-ductile concrete – Material design concept and testing. *Ultra-ductile concrete with short fibres – Development, Testing, Applications*, V. Mechtcherine (ed.), ibidem-Verlag, Stuttgart: 11-36.
- Mechtcherine, V. & Schulze, J. 2006. Testing the behaviour of strain hardening cementitious composites in tension. *Int. RILEM Workshop on HPRCC in Structural Applications*, Honolulu, May 2005, G. Fischer & V. C. Li (eds.), RILEM Publications S.A.R.L., PRO 49: 37-46.